Desalination and Water Treatment
www.deswater.com
doi: 10.1080/19443994.2015.1082941

57 (2016) 9993–10002
May

Taylor & Francis
Taylor & Francis Group

Experimental study on overall heat transfer coefficient of seawater on three tube arrangements for horizontal-tube falling film evaporator

Xingsen Mu[a,*], Shengqiang Shen[a], Yong Yang[a], Gangtao Liang[a], Xue Chen[a], Jili Zhang[b]

[a]*Key Laboratory of Liaoning Province for Desalination, School of Energy and Power Engineering Dalian University of Technology, Dalian 116024, Liaoning, China, Tel. +86 13591366001; email: muxingsen@dlut.edu.cn (X. Mu), Tel. +86 13050505853; emails: zzbshen@dlut.edu.cn (S. Shen), yangyong@dlut.edu.cn (Y. Yang), gtliang@dlut.edu.cn (G. Liang), 230243143@qq.com (X. Chen)*
[b]*School of Civil Engineering Dalian, University of Technology, Dalian 116024, Liaoning, China, email: zjldlut@dlut.edu.cn*

Received 16 November 2014; Accepted 10 August 2015

ABSTRACT

In this paper, two sets of experimental devices have been established for studying the falling film evaporation outside a horizontal tube and condensation inside a horizontal tube, with three different tube arrangements and seawater as the experimental fluid. The rules of the overall heat transfer coefficient (K) are determined by changing saturation temperature (T), Reynolds number (Re), total temperature difference (ΔT), inlet steam velocity (v_s), and vapor quality (x). Experimental results indicate that the overall heat transfer coefficient of the rotated square arrangement (K_{rs}) is higher than that of the triangular arrangement (K_t), and the square one (K_s) is the lowest with less impact on Re, T, ΔT, v_s, or x changing. With Re increasing, the K increases first and then declines, especially when $Re > Re_{cr}$, K_{rs} and K_t are almost the same. The increment of T and ΔT leads to the decreasing of the K, while v_s has little effect on the K. The growth of x contributes a lot to the increment of the K. In the evaporator, the vapor quality contributes a lot in the horizontal direction, while Re is more influential in the vertical direction.

Keywords: Horizontal-tube falling film; Overall heat transfer coefficient; Tube arrangement; Desalination; Seawater

1. Introduction

Desalination, which is an efficient way to explore new water sources, has become an established method to solve the insufficiency of fresh water source. Among all the technology, low-temperature multi-effect distillation (LT-MED) is one of the primary technologies for large-scale desalination equipment, with the advantages of stable operation, high water quality, low cost, and waste heat reuse. Falling film evaporation outside horizontal tube is the main technology adopted in LT-MED, with small heat transfer temperature difference and high heat transfer coefficient. In addition, it is also widely used in the fields of refrigeration engineering, food processing industry, petrochemical industry, etc.

Researchers have done amount of work on horizontal-tube falling film evaporation for several decades. The overall heat transfer coefficient (K) is difficult to measure during the experiment because of the coexistence of the condensation inside the tube and the evaporation outside the tube. With different

*Corresponding author.

working fluids and parameter ranges, the conflicting results have been presented in the published papers.

About the research of spray Reynolds number (Re) on the heat transfer coefficient, Hu and Jacobi [1], Yang and Shen [2], Zeng and Chyu [3] got the same conclusion that the heat transfer coefficient outside the tube (h_o) increases with the Re rising. Fujita and Tsutsui [4,5] stated that h_o declines at the beginning, and then rises with the increment of Re. In our previous research [6], h_o increases first, and then declines with the growth of Re with the influence on the growth of speed and thickness of liquid film concurrently.

The correlativity between the saturation temperature (T) and heat transfer coefficient varies with different experiment liquids. Chang et al. [7] took refrigerating fluid R141b and Mu et al. [8] chose the natural seawater as working fluid. Their researches have indicated that the increment of T results in the decrement of h_o. In the study of Armbruster and Mitrovic [9], Parken et al. [10], and Mu et al. [6], the fresh water was chosen as the working fluid, and the h_o appears escalating trend first and then declining with the growth of Re.

For the effect of the total temperature difference (ΔT) on the heat transfer performance, Fujita and Tsutsui [4], Hu and Jacobi [1], Mu et al. [11] stated that the h_o is almost independent on the total temperature difference (ΔT). The research in Cavallini et al. [12] shows that the increment of ΔT has significant benefits to the increment of the thickness of liquid film inside the tube and the decrement of the local heat transfer coefficient inside the tube (h_i).

About the effect of the inlet steam velocity (v_s) on the heat transfer coefficient, Dobson and Chato [13] reported that the increment of inlet steam velocity (v_s) enhances the heat convection inside the tube, which can improve both the local h_i and the average h_i slightly.

Focused on the vapor quality (x) effect on the heat transfer coefficient, Anowar et al. [14] presented that h_i uniformly declines with the reduction of x. Furthermore, Grauso et al. [15], Quiben et al. [16], Jung et al. [17] found that there is slight benefit to h_i with x decreasing as $x > 0.8$.

To horizontal tube arrays or bundles, the dry-out areas of the bottom tubes are important in heat transfer process. Fujita and Tsutsui [5] have stated that thin falling films are susceptible to heat transfer deterioration accompanied by film breakdown.

The scholars have done many researches on the characteristics of heat transfer both inside and outside the horizontal tube during the falling film process. However, it is quite important to study the different influence factors on K with the same condition, by combining experiments inside and outside the tube together, which is necessary to explore the internal mechanism of falling film evaporation process.

2. Experimental process

2.1. Experimental devices

The overall heat transfer coefficient is calculated based on the results of heat transfer coefficient of inside and outside tubes in two sets of experimental devices. Fig. 1 shows the schematic diagram of experimental device for evaporation outside the horizontal tube. It consists of a heating tank, a high position liquid feeder, a testing cell (evaporator), a metering pot, and two double-pipe condensers.

The seawater is pumped into the high position liquid feeder when it is heated up to the index temperature for the experiment. The partitions and overflow zone are set in high position liquid feeder to remain the working fluids stable (Fig. 1(2)). Then, the fluid goes directly into the evaporator via a rotor flow meter. Uniform spray has many benefits to integrated liquid film outside the heat transfer tube surface, where the vaporization occurs. The vapor will subsequently go into the condenser to be measured while

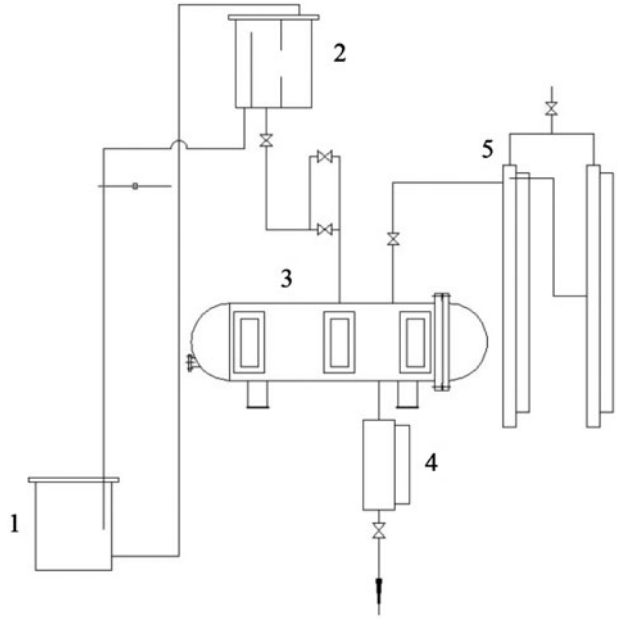

Fig.1. The schematic diagram of evaporation outside a horizontal tube experimental device.
Notes: (1) heating tank, (2) high position liquid feeder, (3) evaporator, (4) measuring pot, and (5) condenser.

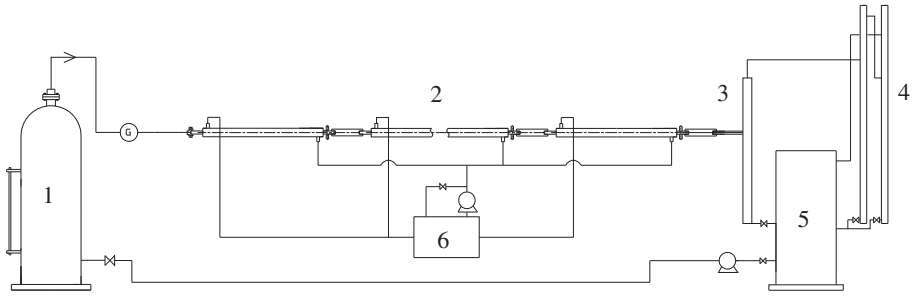

Fig. 2. The schematic diagram of condensation inside a horizontal tube experimental device.
Notes: (1) boiler, (2) testing part, (3) vapor–liquid separator, (4) condenser, (5) reservoir, and (6) cooling water tank.

the unevaporated brine will be discharged out of the system after passing through the measuring pot.

The test tube is made of HAL77–2A aluminum brass with outer diameter of 25.4 mm, inside diameter of 24 mm, and length of 2,000 mm. Heat flux is provided by an electric heater whose power ranges from 0 to 3 kW embedded inside the tube. The saturation temperature (T) and the spray Reynolds number (Re) in this experiment vary from 50 to 70°C and 100 to 600, respectively. More details about this experimental device have been present in the references of this paper [6].

Fig. 2 shows the schematic diagram of experimental device for condensation inside a horizontal tube. It is composed by a boiler, five horizontal test tubes, vapor–liquid separator, two double-pipe condensers, a condensate tank, and a cooling water tank.

The boiler serves to provide the steam for the whole experimental system. The steam exchanges heat with the cooling water by flowing outside the tube, which is pumped from the cooling water tank. The utilized cooling water flows back to the cooling water tank after circulation. Subsequently, the mixture of steam–water flows into the moisture separator to remove the condensation water and entrained water from the steam. The separated water is gathered into the reservoir, and flows back to the boiler for recirculation through the pump ultimately.

The material is still HAL77–2A aluminum brass for the five test tubes, with the outer diameter of 25.4 mm, the inner diameter of 24 mm, and the length of 1,800 mm same as above. The double-pipe condenser is used to replace falling film outside tube. These five test tubes compose five heat transfer test parts, while a 300-mm quartz glass tube is designed to observe the two-phase flow between every two test tubes. The heat transfer performance of single test part has been analyzed by comparing the ratio of steam and fluid. The steam temperature, as conditions selected in this experiment, ranges from 45 to 70°C, and the velocity of inlet steam varies from 20 to 45 m/s, as well as the inlet temperature difference changes between 0.5 and 2°C. More details about the experimental device have been stated in [18].

The heat transfer coefficients of outside tube (h_o) and inside tube (h_i) are measured individually in both experimental systems. The total heat transfer coefficient (K) is calculated by Eq. (1). The parameters including spray density, inlet steam velocity, inlet steam pressure, and vapor quality are changed to simulate the heat transfer process of bundles in experiments.

$$K = \frac{1}{\frac{1}{h_i}\frac{d_o}{d_i} + \frac{d_o}{2\lambda}\ln\frac{d_o}{d_i} + \frac{1}{h_o}} \tag{1}$$

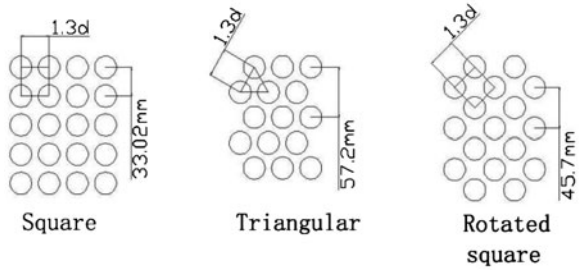

Fig. 3. Tube arrangements.

Table 1
Main ion concentration of experimental seawater

Cation	Concentration (g/L)	Anion	Concentration (g/L)
N_a^+	13.99	SO_4^{2-}	3.04
K^+	0.21	HCO_3^-	0.14
C_a^{2+}	0.38	B_r^-	0.08
M_g^{2+}	3.46	Cl^-	21.6

Table 2
Experimental uncertainties

Position	Instrument	Accuracy
Evaporation outside horizontal tubes	Thermocouple	±0.05℃
	Rotameter	±1.5%
	Testo 240 conductivity measuring instrument	±1 mg/L
	Power governor	±0.5%
	Pressure sensors	±0.2 KPa
Condensation inside a horizontal tube	Thermocouples	±0.05℃
	Pressure sensors	±28 Pa
	Differential pressure gage	±1 Pa
	Gas flowmeter	±1%
	Liquid flowmeter	±0.5%R

2.2. Other details

Fig. 3 presents three different arrangements of the test tubes: square, triangular, and rotated square, which are commonly utilized in practical engineering with a ratio of tube pitch and diameter, $P/D = 1.3$. In the experiment, the vertical tube pitches are selected as 33.02, 57.20, and 45.70 mm, respectively.

The seawater from the Yellow Sea in China is selected as the working fluid with a salinity of 3.4%. Table 1 presents the main ion concentration of the experimental seawater.

The Reynolds number can be calculated by formula (2):

$$Re = \frac{4\Gamma}{\eta} \tag{2}$$

The uncertainty analysis is showed in Table 2.

3. Experimental results and discussions

Different experimental parameters, such as Re, T, ΔT, v_s, and x, on the changes of the overall heat transfer coefficient have been analyzed in the experiment. Specific parameters are shown in Table 3. The dry-out areas will occur in this experimental system with $Re < 60$ showing in our previous research. Whereas the heat transfer tube will be fully wetted visibly because the minimum Re is significantly more than 60 in this experiment.

3.1. Effect of Reynolds number on the overall heat transfer coefficient

The effect of Reynolds number on the overall heat transfer coefficient is discussed under the condition of saturation temperature 60℃, inlet steam velocity 30 m/s, total temperature difference 1.25℃, and vapor quality 0.8.

Table 3
Different working conditions for Figs. 4–8

	Re	T (℃)	ΔT (℃)	v_s (m/s)	x
Fig. 4	166–544	60	1.25	30	0.8
Fig. 5	333	50–70	1.25	30	0.8
Fig. 6	333	60	1.25	20–45	0.8
Fig. 7	333	60	0.5–2	30	0.8
Fig. 8	333	60	1.25	30	0–1

Fig. 4 shows the influence of Reynolds (Re) number on the overall heat transfer coefficient (K) of three tube arrangements. The figure shows that the Re of all the tube arrangements increases rapidly at first then goes stably after that, and decreases slightly at the end. The droplet which has liquid drop impacting film with low frequency is the primary flow pattern when Re is small. The liquid film with weak fluctuation inside is mainly affected by viscous force. With an increase in the Re, K increases, because the fluctuation of liquid film becomes fierce which enhances the convection heat transfer between the film and tube. This figure also shows that K remains constant after Re reaches a specified value. With Re increasing, the thickness of liquid film increases which enhances the influence of conduction resistance and counteracts the effect of convection caused by the fluctuation inside the liquid film. The critical Reynolds number (Re_{cr}) is defined as K reaching the maximum value, where the impact of restraint of thickness of liquid film reaching equilibrium with the intensification of heat convection caused by fluctuation. When the spray Re is larger than Re_{cr}, liquid film goes thicker and conduction resistance plays the leading role. As a result, K declines. In

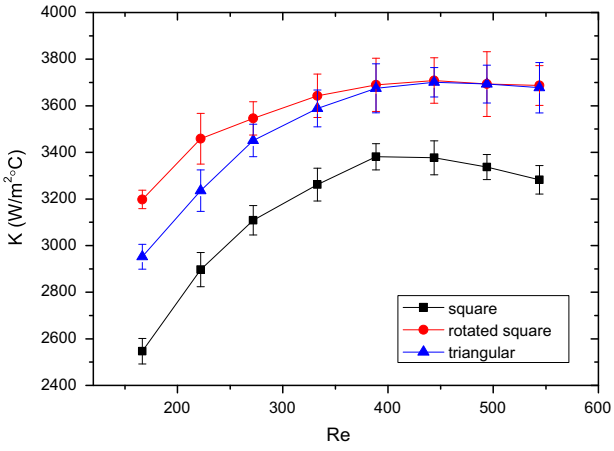

Fig. 4. The influence of Reynolds number (*Re*) on the overall heat transfer coefficient (*K*) with three tube arrangements.

addition, Re_{cr} numbers of the triangular and rotated square arrangements are about 470, while the square one is about 400. Discussing in this paper, the square arrangement has the smallest tube pitch compared with the other two. With respect to Re_{cr}, it is apparent that the square one provides the highest increase speed of the liquid film thickness, resulting in the corresponding increasing thermal resistance, which facilitates the faster achievement to Re_{cr}.

Fig. 4 also shows that the heat transfer coefficient of the triangular arrangement (K_t) is higher than that of the rotated square arrangement (K_{rs}), while the square arrangement is the lowest. On one hand, the velocity of liquid drops draws near $(2gH)^{1/2}$ when liquid drops contact the surface outside the tube. Thus, increasing the tube pitch can improve the liquid velocity. At the same time, the impingement between liquid and tube surface will be intensified, which is beneficial to the convective heat transfer. On the other hand, the increase in vertical tube pitch will also bring about the change of the spray flow pattern [19]. Under the conditions of the experiment, flow pattern varies from drop to jet. As exhibited in Fig. 4, the different spray flow patterns caused by different tube pitches also affected the value of *K* with the same *Re*. Also, it can be figured out that the difference between K_{rs} and K_t is diminishing with an increase in the *Re*. The curves of *K* for two tube arrangements, rotated square and triangular, almost superpose over Re_{cr}, because the flow patterns of rotated square and triangular tube arrangements are quite different when *Re* is low, and the rotated square tube arrangement maintains drop-jet flow pattern, while the triangular tube arrangement acts in jet flow pattern. Whereas the jet flow pattern emerges for the triangular tube arrangement as *Re* increasing. At this time, the differences of the *K* value between the rotated square arrangement and triangular arrangement will decrease.

3.2. Effect of saturation temperature on the overall heat transfer coefficient

The effect of saturation temperature on the overall heat transfer coefficient is discussed under the conditions of Reynolds number 333, inlet steam velocity 30 m/s, total temperature difference 1.25℃, and vapor quality 0.8.

Fig. 5 shows the influence of saturation temperature on the overall heat transfer coefficient (*K*) with three tube arrangements. There is an interesting phenomenon shown in the figure that the *K* declines with an increase in the *T*, which is entirely different with the result adopting fresh water [20] as experimental fluid. The results have been retested in this experimental system and others to verify the accuracy. The phenomenon was caused by thermophysical properties of high-temperature seawater, like viscosity and surface tension [8].

Furthermore, K_t is almost the same with K_{rs}, even a little higher than K_{rs} when *T* varies from 50 to 55℃. It is mainly due to the high viscosity with low *T*. *K* is independent on different vertical tube pitches (tube arrangements of triangular and rotated square) under the condition of the same viscosity, which is difficult for *K* to reveal the difference.

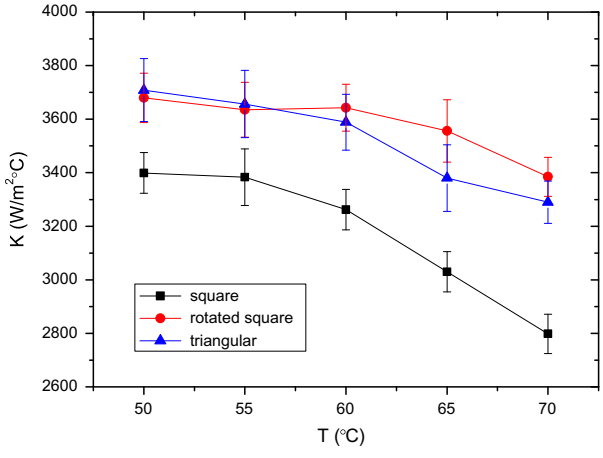

Fig. 5. The influence of saturation temperature (*T*) on the overall heat transfer coefficient (*K*) with three tube arrangements.

3.3. Effect of inlet steam velocity on the overall heat transfer coefficient

The effect of inlet steam velocity on the overall heat transfer coefficient is discussed under the conditions of Reynolds number 333, total temperature difference 1.25℃, and vapor quality 0.8.

Fig. 6 shows the influence of inlet steam velocity on the overall heat transfer coefficient (K) with three tube arrangements. From Fig. 6, it can be found that the value of K reaches a plateau as v_s increasing. Actually, the increase in v_s causes the increase in heat flux for the situation inside the tube. Whereas the heat flux has no effect on h_o in our previous study [6]. For the situation inside the tube, the increase in v_s contributes to the fluctuation of condensation water surface, which slightly enhances the heat transfer coefficient. With this situation, we can hardly use K to represent the influence on heat transfer. As a consequence, it can be considered that the effect v_s on K can be ignored.

3.4. Effect of total temperature difference on the overall heat transfer coefficient

The effect of total temperature difference on the overall heat transfer coefficient is discussed under the conditions of Reynolds number 333, inlet steam velocity 30 m/s, and vapor quality 0.8.

Fig. 7 exhibits the influence of total temperature difference (ΔT) on the overall heat transfer coefficient (K) with three tube arrangements. As shown in Fig. 7, for all three different tube arrangements, K declines with ΔT increasing. The heat transfer coefficient inside the tube h_i consists of the local heat transfer coefficient from steam and condensation region. The amount of local condensed water from steam region increases with ΔT rising, which leads to the rising of the liquid film thickness inside the tube and thermal conduction resistance increasing, and declining the local heat transfer coefficient of steam region. In the condensation region, ΔT has slight impact on the local heat transfer coefficient. With combined impacts of these two regions, h_i eventually declines with the increase in ΔT. With respect to the heat transfer outside the tube, the increase in ΔT results in the rise of heat exchange amount. It will place an increase on the spray Re of the heat transfer tubes at the bottom in a large-scale evaporator with multiple rows. Furthermore, it will decrease the K finally. Nevertheless, the increase in heat transfer amount almost does not affect h_o under conditions of this experiment. Thus, the increase in ΔT leads to the decrease in K.

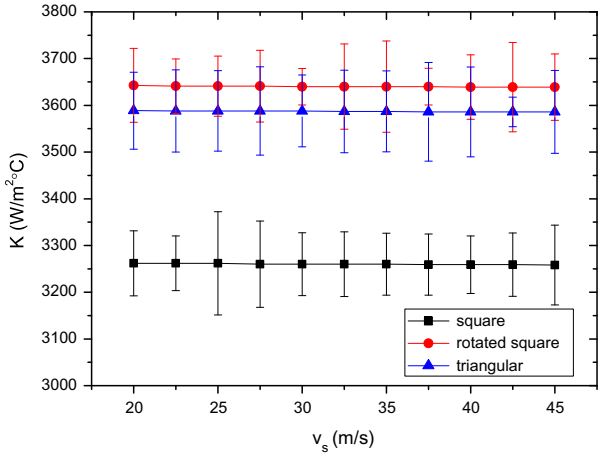

Fig. 6. The influence of inlet steam velocity (v_s) on the overall heat transfer coefficient (K) with three tube arrangements.

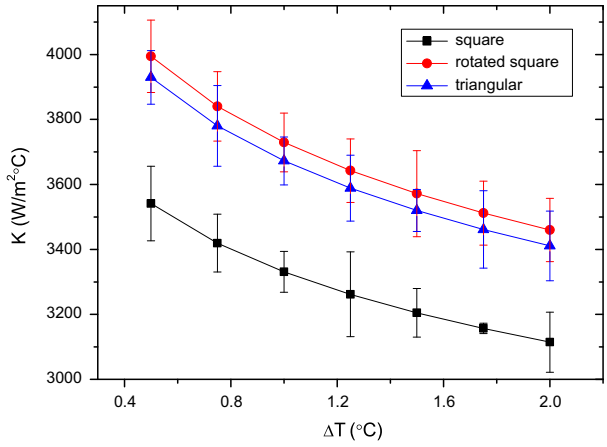

Fig. 7. The influence of total temperature difference (ΔT) on the overall heat transfer coefficient (K) with three tube arrangements.

3.5. Effect of local vapor quality on the overall heat transfer coefficient

The effect of local vapor quality on the overall heat transfer coefficient has been discussed under the conditions of Reynolds number 333, inlet steam velocity 30 m/s, and saturation temperature 60℃.

Fig. 8 shows the influence of local vapor quality (x) on the overall heat transfer coefficient (K) with three tube arrangements. As shown in the figure, K increases with the increment of x. In the process of heat transfer inside the tube, ratio of steam region to condensate region is relative to x, and it rises when x increases. It can be figured out through research in

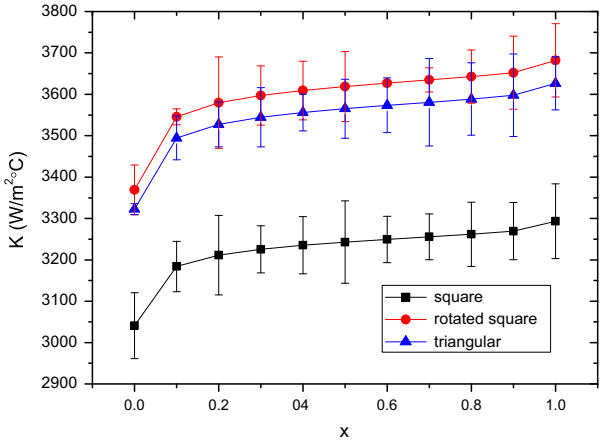

Fig. 8. The influence of local vapor quality (x) on the overall heat transfer coefficient (K) with three tube arrangements.

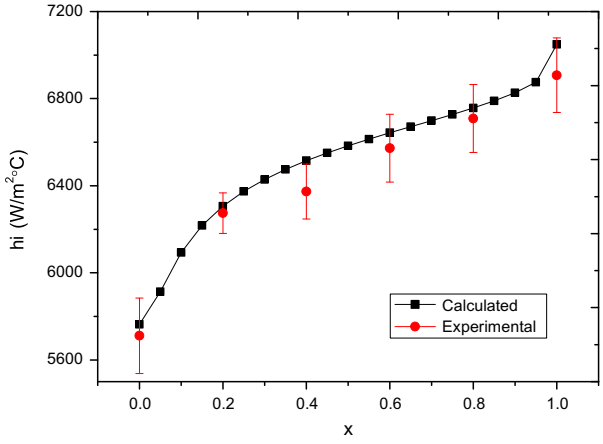

Fig. 10. The Comparison between calculated results and test results of h_i.

[18] that the local heat transfer coefficient of steam region is obviously larger than that of condensation region. Hence, K will get larger with h_i increasing.

4. Space distribution of the K in the evaporator

According to the data from two experiment systems, the different space distributions of the overall heat transfer coefficient (K) of the evaporator with three tube arrangements have been calculated, respectively. The results have met well with experimental data, and the maximum error was 7% (shown in Figs. 9 and 10). The heat transfer tube bundle in the evaporator is composed of 50 columns and 100 rows. Each tube is made of aluminum brass with an outer diameter of 25.4 mm, inside diameter of 24 mm, and length of 10,000 mm. Three different tube arrangements are also considered in the calculation, respectively, with the other conditions, for instance, spray Re of the tubes at the top of 333, saturation temperature of 60°C, saturated steam inlet velocity at 30 m/s, temperature difference of 1.25°C as well as inlet vapor quality of 1. The minimum Re of bottom tubes in this evaporator is around 230, to keep tubes fully wetted.

Figs. 11–13 show the distribution of K inside the evaporator with three different tube arrangements. As shown in all of the three figures, K keeps decreasing

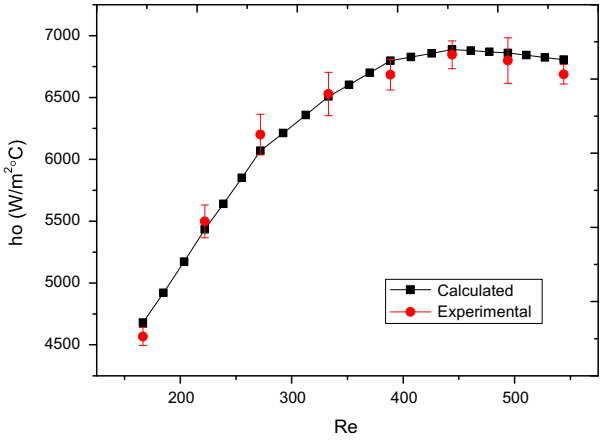

Fig. 9. The Comparison between calculated results and test results of h_o.

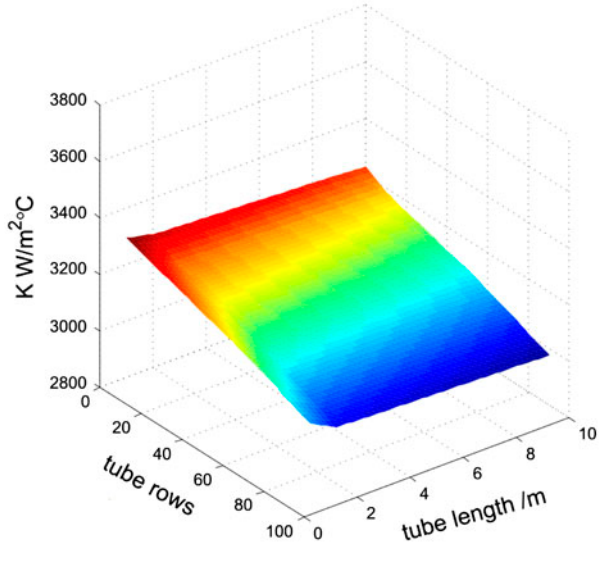

Fig. 11. Space distribution of the overall heat transfer coefficient (K) in the evaporator with square tube arrangement.

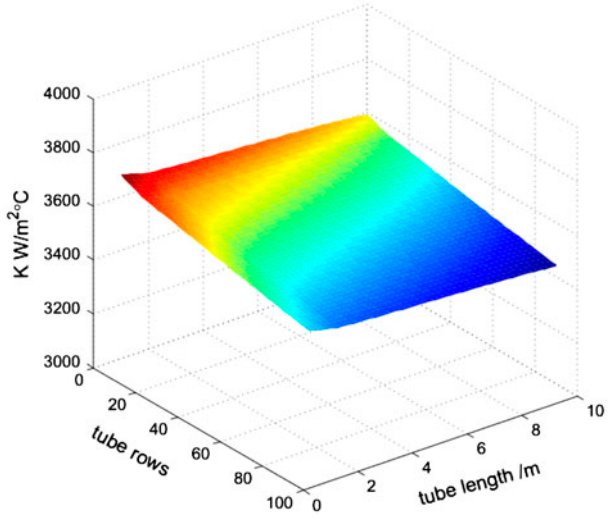

Fig. 12. Space distribution of the overall heat transfer coefficient (K) in the evaporator with rotated square tube arrangement.

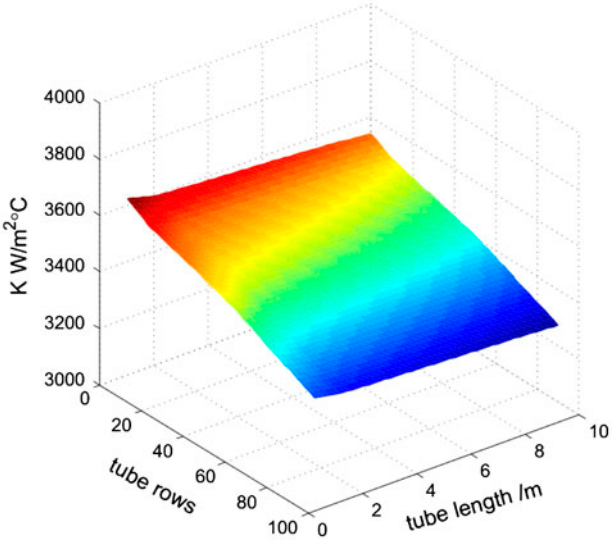

Fig. 13. Space distribution of the overall heat transfer coefficient (K) in the evaporator with triangular tube arrangement.

along the tube. The K of the tubes at top row is mainly influenced by x. As it keeps condensing inside the tube, K is decreasing caused by the decline of x. The K of other rows is influenced by spray volume and x, which keeps decreasing along the tubes. The evaporation along the tubes at the top row has significant impact on the spray volume of the next row tubes, as a result, the farther away from the steam inlet, the lower the evaporation and K, which provides the larger spray volume along the next row tubes. On the basis of the previous researches, K rises with the Re increasing when Re ranges from 100 to 333. Under the combination of the two opposite factors, K decreases along the tube, as shown in the figures. It can be considered that under conditions of this experiment, the effect of x is greater than Re on K.

Furthermore, K also decreases along with the direction of growing tube rows. In the steam inlet region, x remains the same with the increasing tube rows, while Re decreases because of the different evaporation outside the tube at the top row, which leads to the decline of K. For the other regions, the growing tube rows result in the rise of x and the reduction of Re. In a word, it shows that under conditions of this experiment, K is affected much more by Re than x along the direction of growing tube rows.

Table 4 presents the decrease percent of heat transfer coefficient (K) in different regions on the tubes from top to bottom row of three tube arrangements. Table 4 indicates that K of rotated square tube arrangement has the least decrease regardless of the region of inlet, middle, or outlet. According to the previous analysis, the impact of K is quite obvious on different liquid patterns. In addition, the K of triangular and rotated square tube arrangements decline along the tube, while the square tube arrangement rises at first and then declines. The square tube arrangement has the least quality of condensate inside the tube in the same position comparing with other two arrangements, because the square arrangement has the smallest K_s rather than the triangle and rotated square tube arrangements.

As shown in Table 4, K_{rs} is the highest and K decreases a little along with the increasing tube rows. Irrespective of the density of tube arrangement, the

Table 4
Decrease percent of K in different regions on the tubes from top to the bottom row with three tube arrangements

	Inlet region (%)	Middle region (%)	Outlet region (%)
Square	7.31	8.06	7.84
Rotated square	4.51	4.35	4.18
Triangular	8.13	7.82	7.54

rotated square tube arrangement is more suitable to the falling film evaporators on horizontal tubes with multiple tube bundles.

5. Conclusions

Natural seawater is adopted as the experiment fluid in the experiment. On the basis of the data from the two sets of experiment devices, the range of K with different factors has been compared of triangular, square, and rotated square tube arrangements. Besides, the space distribution of K inside the evaporator has been also discussed in different tube arrangements. Main conclusions can be drawn as follows:

(1) Under conditions of this experiment, it is the same result that $K_{rs} > K_t > K_s$ no matter how Re, T, ΔT, v_s, or x change.
(2) With Re increasing, K increases first and then declines, especially when $Re > Re_{cr}$, K_{rs} and K_t is almost the same.
(3) With T increasing, K decreases, and when T is low, where K_{rs} and K_t are roughly the same.
(4) With ΔT increasing, K decreases.
(5) Under conditions of this experiment, v_s has little effect on K.
(6) K is obviously affected a lot by x under conditions of this experiment, and K increases with x rising.
(7) In the evaporator, x has main impact on K along the tube, while Re contributes most to K along the direction of growing tube rows. K_{rs} decreases the least along with the direction of growing tube rows.

Acknowledgment

The authors are gratitude for the financial supported by Chinese National Natural Science Foundation Project Numbers 51406024, 51336001, China Postdoctoral Science Foundation funded project (2014M551079), and Fundamental Research Funds for the Central Universities (DUT15LAB14).

Nomenclature

K	—	total heat transfer coefficient (kW/m^2℃)
h	—	heat transfer coefficient (kW/ m^2℃)
Re	—	Reynolds number
T	—	saturation temperature (℃)
ΔT	—	temperature difference (℃)
v_s	—	inlet steam velocity (m/s)
x	—	vapor quality
d	—	tube diameter
λ	—	thermal conductivity
subscripts		
o	—	outside tube
i	—	inside tube
t	—	triangular pitch
s	—	square pitch
rs	—	rotated square pitch
cr	—	critical

References

[1] X. Hu, A. Jacobi, The intertube falling film: Part 2—Mode effects on sensible heat transfer to a falling liquid film, J. Heat Transfer 118 (1996) 626–633.
[2] L. Yang, S. Shen, Experimental study of falling film evaporation heat transfer outside horizontal tubes, Desalination 220 (2008) 654–660.
[3] X. Zeng, M. Chyu, Evaporation heat transfer performance of nozzle sprayed ammonia on a horizontal tube, J. ASHRAE. 101 (1995) 317–324.
[4] Y. Fujita, M. Tsutsui, Evaporation heat transfer of falling films on horizontal tube. Part 2: Experimental study, J. Heat. Trans. Jpn. 24 (1995) 17–31.
[5] Y. Fujita, M. Tsutsui, Experimental investigation of falling film evaporation on horizontal tubes, J. Heat Trans. Jpn. 27 (1998) 609–618.
[6] X. Mu, S. Shen, Y. Yang, X. Liu, Experimental study of falling film evaporation heat transfer coefficient on horizontal tube, Desalin. Water Treat. 50 (2012) 310–316.
[7] T. Chang, C. Lu, J. Li, Enhancing the heat transfer performance of triangular-pitch shell-and-tube evaporators using an interior spray technique, Appl. Therm. Eng. 29 (2009) 2527–2533.
[8] X. Mu, Y. Yang, S. Shen, G. Liang, L. Gong, Experimental study of heat transfer characteristics for horizontal tube falling film evaporation, ASME 2012 Summer Heat Transfer Conference, Puerto Rico, USA, 2012.
[9] R. Armbruster, J. Mitrovic, Heat transfer in falling film on a horizontal tube, in: Proceedings of the National Heat Transfer Conference, Porland, 1995.
[10] W. Parken, L. Fletcher, V. Sernas, Heat transfer through falling film evaporation and boiling on horizontal tubes, J. Heat Transfer 112 (1990) 744–750.
[11] X. Mu, X. Liu, S. Shen, X. Chen, L. Gong, Experimental study of some elements influencing heat transfer coefficient of horizontal-tube falling film evaporation, J. Acta Energiae Solaris Sinca 35 (2014) 830–834.
[12] A. Cavallini, G. Censi, D. Del Col, Experimental investigation on condensation heat transfer and pressure drop of new HFC refrigerants (R134a, R125, R32, R410A, R236ea) in a horizontal smooth tube, Int. J. Refrig. 24 (2001) 73–87.
[13] M.K. Dobson, J.C. Chato, Condensation in smooth horizontal tubes, J. Heat Transfer 120 (1998) 193–213.
[14] M.D. Anowar, A. Hossaina, Y. Onaka, A. Miyara, Experimental study on condensation heat transfer and pressure drop in horizontal smooth tube for R1234ze (E), R32 and R410A, Int. J. Refrig. 35 (2012) 927–938.
[15] S. Grauso, R. Mastrullo, A.W. Mauro, Flow pattern map, heat transfer and pressure drops during

evaporation of R-1234ze(E) and R134a in a horizontal, circular smooth tube: Experiments and assessment of predictive methods, Int. J. Refrig. 36 (2013) 478–491.
[16] J.M. Quiben, J.R. Thome, A. Cavallini, Flow pattern based two-phase frictional pressure drop model for horizontal tubes, Part II: New phenomenological model, Int. J. Heat Fluid Flow 28 (2007) 1060–1072.
[17] D. Jung, K. Song, Y. Cho, S. Kim, Flow condensation heat transfer coefficients of pure refrigerants, Int. J. Refrig. 26 (2003) 4–11.
[18] S. Shen, R. Liu, Condensation character of a stratified flow inside a horizontal tube, Desalin. Water Treat. 33 (2011) 218–223.
[19] X. Hu, A. Jacobi, The intertube falling film: Part 1-Flow characteristics, mode transitions, and hysteresis, J. Heat Transfer 118 (1996) 616–625.
[20] S. Shen, G. Liang, Y. Guo, R. Liu, X. Mu, Heat transfer performance and bundle-depth effect in horizontal-tube falling film evaporators, Desalin. Water Treat. 51 (2013) 830–836.